ELSEVIER

Sensors and Actuators A 88 (2001) 104–111

SENSORS AND ACTUATORS A PHYSICAL

www.elsevier.nl/locate/sna

# Miniature valveless pumps based on printed circuit board technique

Nam-Trung Nguyen*, Xiaoyang Huang

*School of Mechanical and Production Engineering, Nanyang Technological University, 50 Nanyang Avenue, Singapore 639798, Singapore*

Accepted 4 September 2000

**Abstract**

This paper presents a new concept of designing microfluidic devices. By using printed circuit board (PCB) as the substrate material, miniature valveless pumps have been successfully developed. The pump can be operated as a single diffuser/nozzle pump or a peristaltic pump, and can delivery a maximum flow rate of 3 ml/min. The detailed design, fabrication, and characterization of the pumps are described in the paper. The PCB technique presents a low-cost and flexible alternative for small-scale production of microfludic devices.


*Keywords:* Printed circuit board; Microfluidic system; Micropumps; Piezoelectric actuators

## 1. Introduction

Microfluidics has been established as a new engineering discipline with a huge scientific and commercial potential. In the last decade, research on microfluidic devices and fluidic phenomena in micro scale became a strategic topic of the international research community [1,2]. Numerous fluidic components have been realized in silicon technology. The most common components are micropumps, valves, flow sensors, separators and mixers [3–5].

The new concept presented in this paper is a response to recent development trends of microfluidic systems. Firstly, complex microfluidic systems (lab-on-a-chip, micro total analysis system) require high cost in development and production because of the cost of mask making and clean room processes. This is only cost-effective for multi-purpose systems with a large market. Secondly, the problem of expensive packaging is still not solved. Nowadays the cost of packaging can make up to 75% of the cost of the whole microfluidic system [1]. The cost calculations discussed below are derived from those of classical microelectronics [6]. The cost of silicon based microfluidic system $c_{\text{system}}$ is calculated from the cost of a die $c_{\text{die}}$, the testing cost $c_{\text{testing}}$, the packaging cost $c_{\text{packaging}}$ and the final test yield $\alpha_{\text{final}}$:

$$c_{\text{system}} = \frac{c_{\text{die}} + c_{\text{testing}} + c_{\text{packaging}}}{\alpha_{\text{final}}} \tag{1}$$

While the packaging cost $c_{\text{packaging}}$ of a microfluidic system is critically high due to the lack of micro-macro interconnection standards, the cost of a die $c_{\text{die}}$ is also high because of the relatively large size of the system and consequently the small number $N$ of dies per wafer:

$$c_{\text{die}} = \frac{c_{\text{wafer}}}{N\alpha_{\text{die}}} \tag{2}$$

The die yield per wafer $\alpha_{\text{die}}$ is proportional to the complexity of the whole system $\beta_{\text{system}}$:

$$\alpha_{\text{die}} \sim \frac{1}{\beta_{\text{system}}} \tag{3}$$

The Eqs. (1)–(3) show that the cost of a silicon based microfluidic system could be much higher than a traditional microelectronic chip.

In order to make the cost of a microfluidic system acceptable, alternative fabrication methods like plastic molding and hot embossing can be used. Our approach used printed circuit board (PCB) as a substrate for electronic components as well as fluidic elements. Table 1 compares some common parameters of MEMS-technology, PCB-technology and those required by microfluidic systems. The comparison shows that PCB can be the solution for systems with no critically small structures.

The above mentioned cost problems may be solved by using PCB as a substrate for electronic circuits as well as for microfluidic components. Fig. 1 describes our design methodology. A micro fluidic system consists of functional modules. A functional module has several functional components (pumps, valves, sensors, etc.), and a functional

* Corresponding author. Tel.: +65-790-4956; fax: +65-791-1859.
*E-mail address*: namtrungnguyen@yahoo.com (N.-T. Nguyen).

0924-4247/01/$ – see front matter 
PII: S0924-4247(00)00500-8

Table 1
Typical parameters of silicon-MEMS, PCB and microfludic devices

| Parameters | Silicon-MEMS | PCB | Microfludics |
|---|---|---|---|
| Resolution | ~5 micron | ~100 micron | 50 micron–10 mm |
| Clean room class | 100–1000 | 1000–10000 | Typ. 1000 |
| Electronic compatibility | Typ. 4 metal layers | 4–20 metal layers | Typ. 1 metal layer |
| Bonding techniques | Anodic, diffusion, adhesive | Eutectic, lamination (adhesive) | Anodic, diffusion, adhesive |

component is designed with different functional elements (actuators, channels, etc.). Lammerink et. al. [7] presented a demonstrator of a microfluidic system with channels milled in PCB, they introduced the term mixed circuit board (MCB). Silicon components were glued to the fluidic board. Recently, research efforts have been made in order to integrate passive fluidic elements (channels, orifices) and sensors into the PCB [8,9].

Pumps are important components for liquid and sample transport in microfluidic systems. The role of the pumps in those systems is similar to the power supply in an electronic system. Because of its robust and reliable design, miniature pumps also have their place in aerospace applications [10]. Therefore, miniature pumps were selected as first objects of our study on PCB-based microfluidic systems.

Micromachined pumps are classified by actuating principles (piezoelectric, pneumatic, thermopneumatic, thermomechanic, electrostatic), pump principles (reciprocating, peristaltic, electrohydrodynamic, electroosmotic, ultrasonic) or even principle with check-valves and without them (valveless) [3–5]. Because of the simple fabrication, valveless pumps have been attracted the attention of microfluidics research community. Valveless pumps are divided into the following categories:

- Peristaltic pumps which can have a maximum flow rate of 100 μl/min for water [11].
- Diffuser/nozzle and valvular conduits pumps which can generate a maximum flow rate of 2000–3000 μl/min water [12,13].
- Ultrasonic pumps which induce acoustically a flow rate on the order of 10 μl/min [14,15].

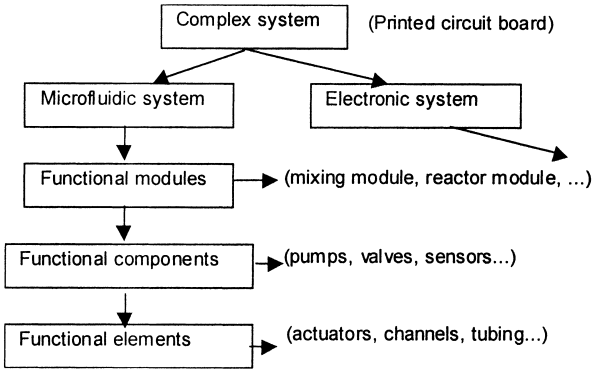


Fig. 1. Design methodology for a complex microfluidic system with fluidic and electric subsystems.

- Electroosmotic and electrophoresis pumps which can move liquids with a velocity <1 mm/s. Depending on the capillary diameter and the applied voltage, a flow rate of several hundred nanoliter per minute can be achieved [16].

The first two categories are simple and do not required special technologies. Hence, the valveless PCB-pumps presented in this paper are based on the peristaltic principle and diffuser/nozzle principle.

## 2. Diffuser/nozzle pump

### 2.1. Fabrication

The development of the diffuser/nozzle pump was our first effort to sink the packaging cost by combining functional elements (diffuser/nozzle) with packaging materials (PCB, inlet/outlet tubes) (Fig. 2). Fig. 2a illustrates the

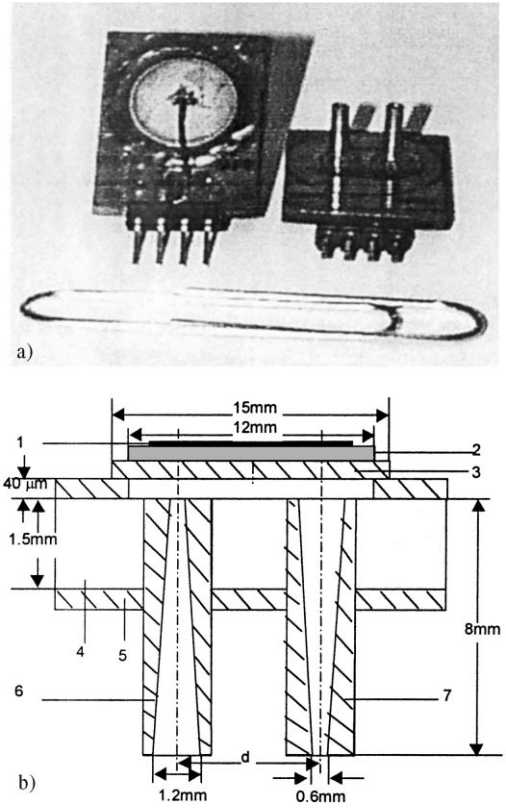


Fig. 2. The diffuser/nozzle pump (not to scale): (a) assembled pump; (b) pump structure ((1): conductive layer, (2): piezoelectric disc, (3): brass plate, (4): PCB-substrate, (5): copper layer, (6): outlet tube, (7): inlet tube).

finished diffuser/nozzle pump. Commercial PCB with coated positive photo resist was used as substrate material. The copper layer on both sides had a thickness of about 40 microns. The pump chamber was etched in the copper layer by iron chloride solution. Afterward, inlet and outlet holes were drilled into the substrate. The piezo disc was soldered directly to the copper layer of the PCB. The inlet and outlet copper tubes are also diffuser/nozzle elements. The diffuser structure was fabricated using classical cutting techniques. The two tubes were then soldered to the backside of the PCB, Fig. 2b. For large-scale production, inlet and outlet tube can be made of plastic and pressed into the holes in the PCB. The self-fitting tubes will not require adhesive sealing or soldering.

### 2.2. Piezoelectric actuator disc

In order to keep the design simple, commercially available piezo discs were selected as actuators. These piezo discs are normally used as buzzers in electronic equipment.

The piezo disc consisted of a piezoelectric ceramic layer glued on a brass disc. Our pump design used the brass disc as the pump membrane. The brass disc had a diameter of 15 mm and a thickness of 95 μm. The piezoelectric layer had a diameter of 12 mm and a thickness of 175 μm. With a maximum drive voltage of 200 V, the maximum electrical field strength was 1.1 kV/mm which was lower than the break down field of most common piezoelectric materials (>2 kV/mm).

In this paper, we define the top electrode of the piezo disc as the voltage terminal and the brass disc as the ground terminal. The square wave signal at the voltage terminal has the high potential level $V+$ and a low potential $V-$.

The electric field applied on the piezoelectric layer induced an expanding strain in the disc perpendicular to the electric field and a contracting strain in the direction of the disc thickness (assuming that the piezoelectric coefficient $d_{31}$ is negative and $d_{33}$ is positive). Since the piezoelectric layer was tightly glued to the brass disc, there were reacting forces from the brass disc opposing the expansion of the piezoelectric layer. This motional restriction caused the deflection of the disc. Our work focused on the experimental characterization of the time-dependent bending of the piezo disc.

The disc deflection can be measured directly with a laser auto-focus system (UBM) or another instruments. In our case, the piezo disc was characterized by a laser vibrometer (Polytech) available in our lab. The piezo disc of the pump shown in Fig. 2 was investigated. The piezo disc was soldered to the PCB. Fig. 3 shows the dynamic characteristics of the center of the piezo disc. Since the vibrometer only measured the vibration velocity (Fig. 3a), the disc deflection was calculated based on the velocity and time data. Using this measurement system, the absolute deflection can not be measured because of the unknown initial condition. The results of the disc deflection were, therefore,

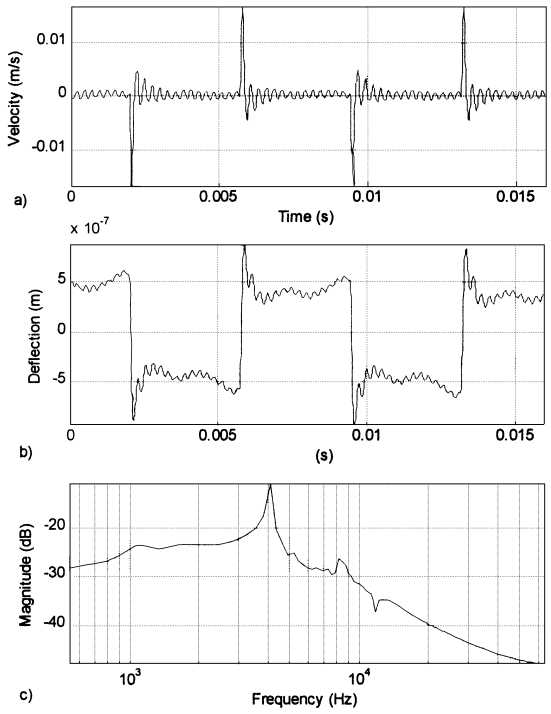


Fig. 3. Results of vibration measurement ($V = \pm 30$ V, pump chamber filled with air): (a) velocity, (b) displacement, (c) transfer function of the piezo disc.

corrected by a first-order fitting function which eliminated the offset and centers the deflection on zero (Fig. 3b). Based on the deflection data and the excitation signal, the transfer function of the disc was calculated (Fig. 3c). The transfer function identifies the piezo disc as a typical second-order system with a resonant frequency of about 4 kHz. Fig. 4

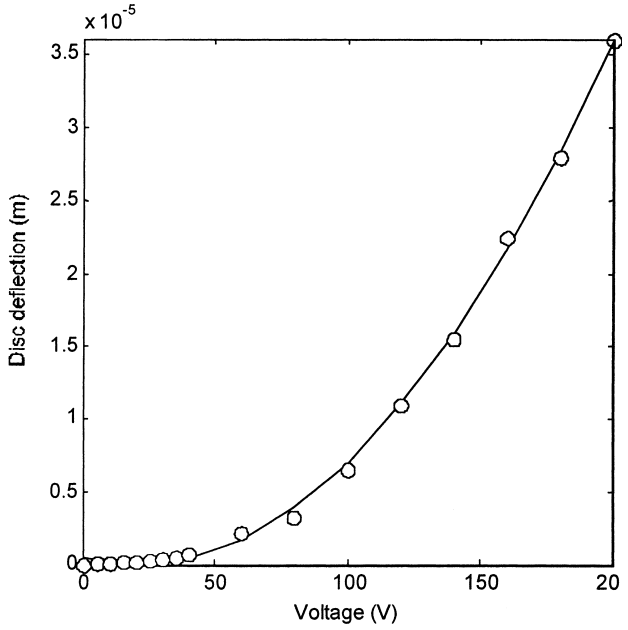


Fig. 4. The deflection as function of voltage (○: measured data, solid line: fitting function $dz = 0.0011\,V^2 + 0.0477\,V + 0.5495$).

shows the membrane deflection versus the applied voltage. The circles in this figure represent the measured results, the solid line is a polynomial fitting function of second-order. The deflection-voltage characteristics show a typical parabolic behavior.

### 2.3. Simulation and characterization

A numerical simulation of the pump was performed. The simulation used a commercial CFD solver (CFD-ACE). The membrane deflection was described as a moving wall in a moving grid model which was reshaped in each calculating time step. The interaction between the fluid and the pump membrane was neglected. The deformation of the pump membrane $dz(r, t)$ was calculated in an user routine by using the Timoshenko's theory of thin circular plates with small deflection

$$dz(r,t) = A_0(t)\left[1 - \left(\frac{r}{R}\right)^2\right]^2 \quad (1)$$

where $r$ is the radial coordinate, $R$ the radius of the piezo disk and $A_0$ the time-dependent deflection of the piezo disc taken from experiments described in Section 2.2.

Different actuating schemes can be applied for the model: sinusoidal or square-wave deflection. Fig. 5a and b shows the typical results of velocity field of the pump model in the supply mode and the pump mode. The pumping effect from right to left can be seen clearly. Our detailed results of the transient simulation of diffuser/nozzle pumps was reported in [17].

The pump was tested with water. We used a simple set-up illustrated in Fig. 6. The water level difference between the pump outlet and the reservoir was adjustable in order to carry out the measurement of the back pressure versus flow rate characteristics. The flow rate was calculated from the velocity of the water-air interface at the pump outlet and the tube diameter. The velocity was measured manually by a ruler and a stopwatch. Fig. 7 shows experimental results of the pump performance in terms of flow rate versus drive frequency. During the test, the performance of the pump at

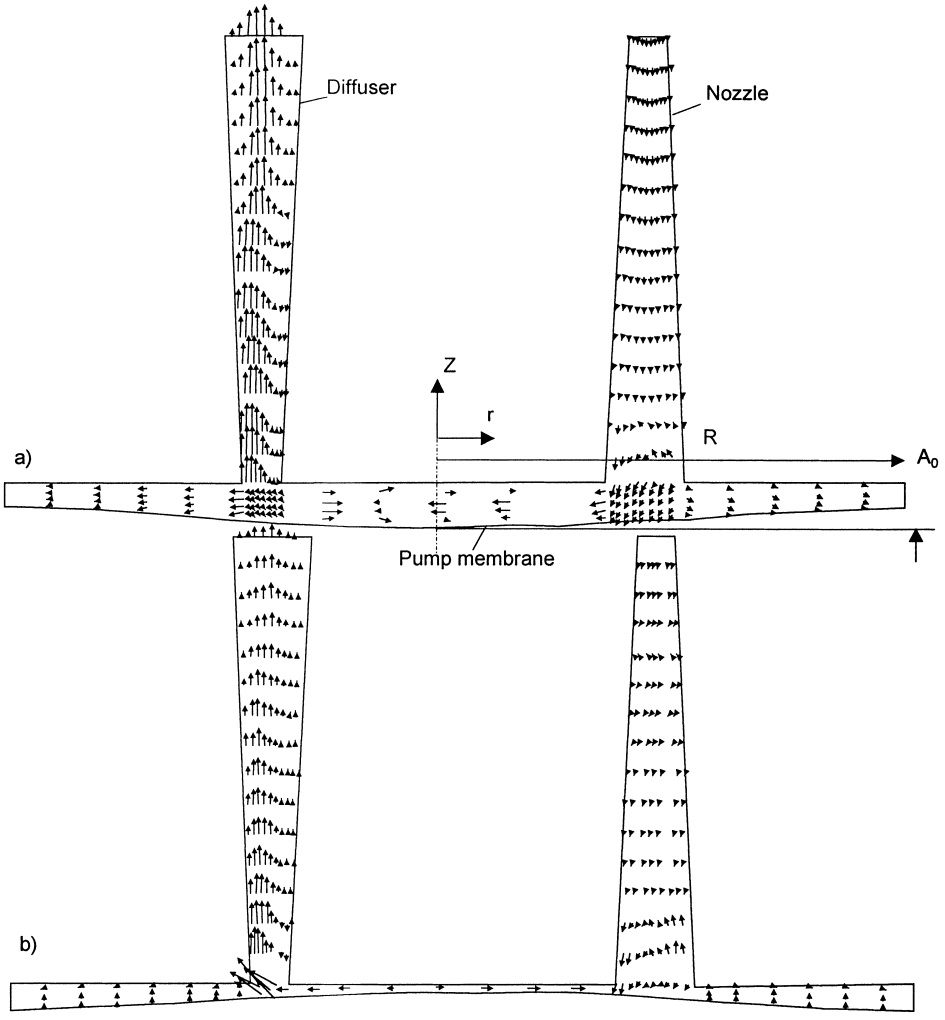


Fig. 5. Simulated velocity field inside the diffuser/nozzle pump in supply mode (a) and pump mode (b) (the pump chamber is enlarged 10 times in $z$-axis for the explanation purpose).

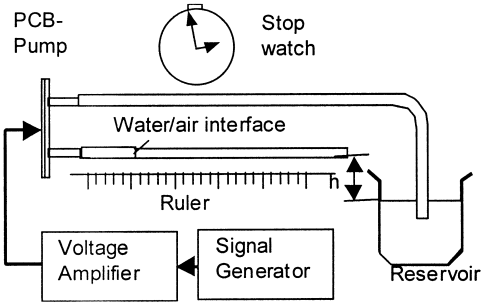


Fig. 6. Experimental set-up.

high drive frequencies was found not as good as that at low frequencies due to the inertia of the system. Besides, a high temperature was detected in the pump chamber when the pump operated at high frequencies which was caused by the mechanical work of the piezo disc dissipated into the thermal energy.

Fig. 8 shows the characteristics of the flow rate versus disc deflection at a constant drive frequency of 100 Hz. The results of two pumps with different distances between inlet and outlet are illustrated. We can see that the pump with inlet and outlet closer to disc center have a better pump performance. The deflection was calculated from the drive voltages and the fitting function described in Fig. 4. The influence of the back pressure on the flow rate was investigated by changing the height between the measurement tube and the water level in the reservoir. At the end of the next section, the back pressure — flow rate characteristics of the diffuser/nozzle pump is compared with that of the peristaltic pump.

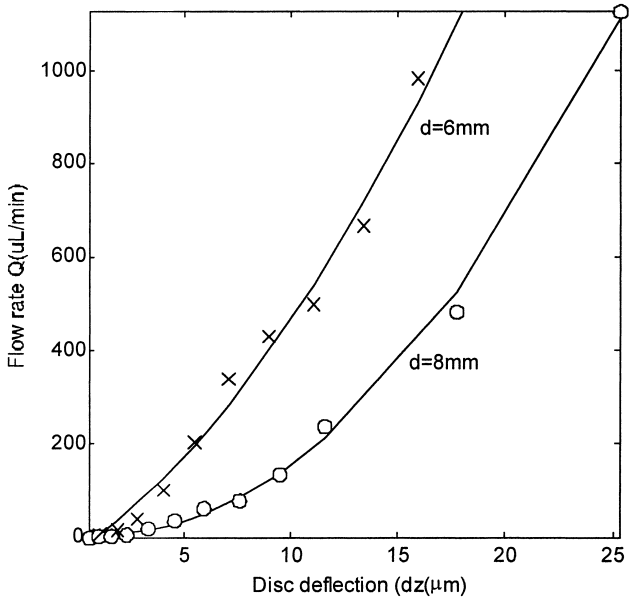


Fig. 8. Flow rate vs. drive disc deflection (water, $f = 100$ Hz, inlet/outlet distances of $d = 6$ and $d = 8$ mm).

## 3. Peristaltic pump

### 3.1. Operation principle and fabrication

In contrast to diffuser/nozzle pumps, peristaltic pumps synchronize several piezo discs in a wave-like motion. This peristaltic motion transports the fluid in one direction and requires no diffuser/nozzle. Classical peristaltic pumps generate the wave-like motion by a wheel with roles along the

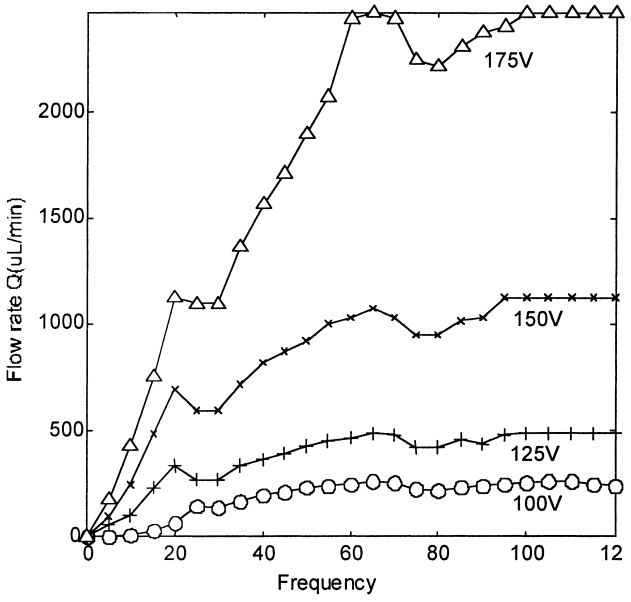


Fig. 7. Pump performance with different frequencies and voltages of drive signals (water, 8 mm inlet/outlet distance).

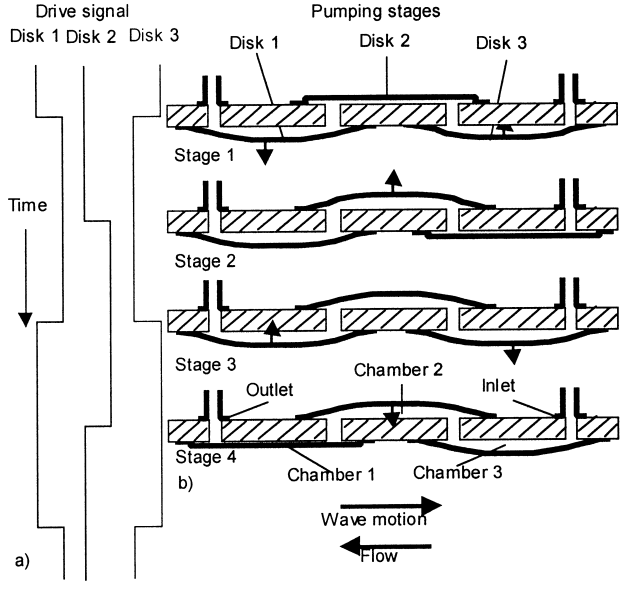


Fig. 9. Operation principle of the peristaltic pump: (a) signaling scheme, (b) the corresponding pumping stages.

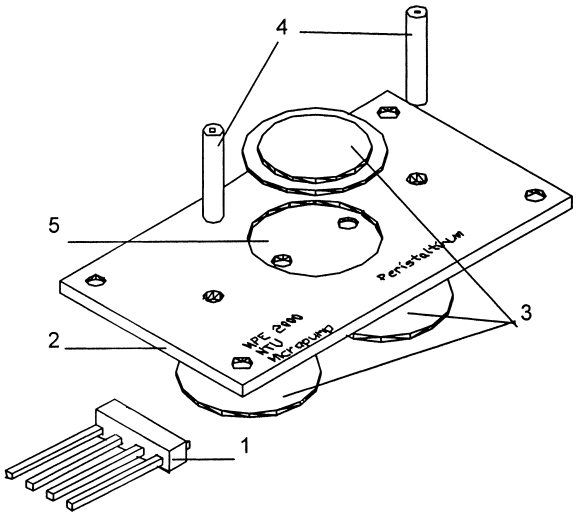


Fig. 10. The peristaltic pump: (1) header for electric interconnection, (2) PCB, (3) piezo discs, (4) inlet/outlet tubes, (5) pump chamber etched in the copper layer.

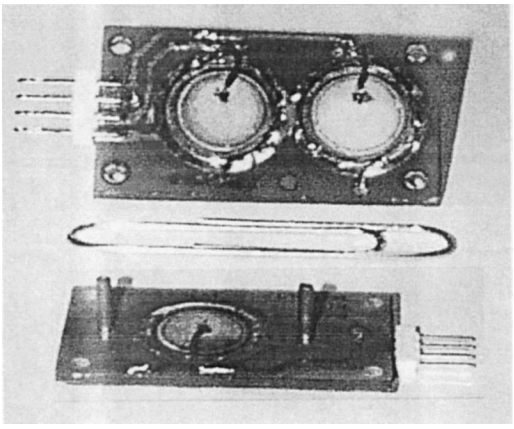

Fig. 11. The finished peristaltic pump.

circumference. The roles press on a flexible silicon rubber tube and cause the wave-like motion when the wheel rotates. The micromachined peristaltic pump reported in [10] used active valves at the outlet and the inlet, the signaling scheme did not describe a true wave-like motion.

In our design, a minimum number of three piezo discs are required for a wave-like motion. Fig. 9 illustrates the signaling scheme for the three piezo discs in our design. The piezo discs are actuated by square-wave signals. The second and the third signals have a phase shift of 90° and 180° to the first signal. In Fig. 9, the wave motion goes from left to right while the fluid flows from right to left. When the first signal is switched to high level, the first disc sucks the fluid from the second disc into the first pump chamber while the third disc is closed and pushes the fluid to the second chamber (stage 1, Fig. 10b). With a 90° phase shift, the second disc is opened and sucks the fluid from the third chamber into the second chamber. Due to its inertia the fluid continues to flow to the outlet. In the third stage, disc 1 is closed and pushes the fluid to the outlet. While the second chamber is still opened, disc 3 sucks the fluid from the inlet into the third chamber. In the last stage of the pumping period, disc 2 pushes the fluid out of the second chamber. The fluid is pushed through the first chamber to the outlet. The process described above will be illustrated with the simulation results presented in the next section.

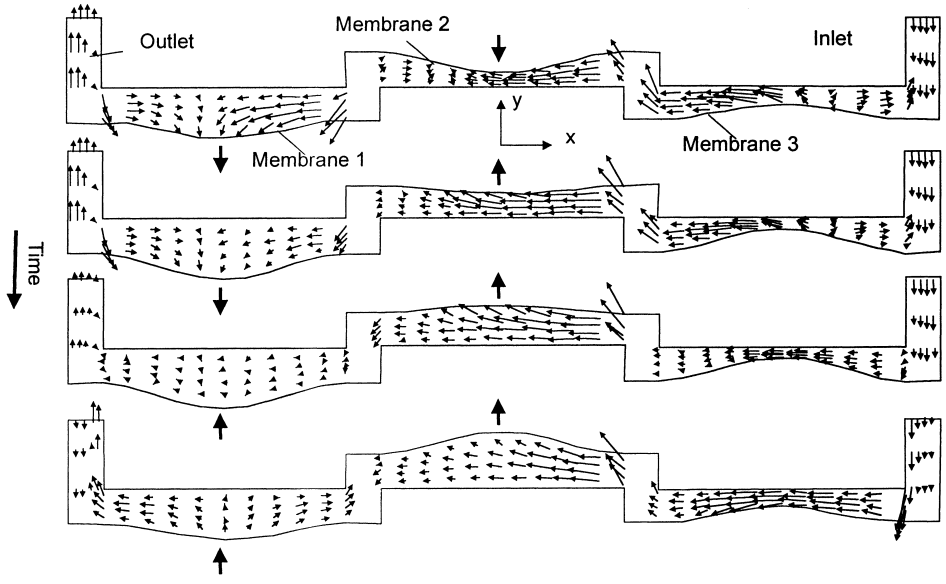


Fig. 12. Results of the velocity field in a simplified model for the peristaltic pump (water, 100 Hz pump frequency, 40-micron maximum deflection. The *y*-axis in this figure is scaled up 50 times. The arrows indicate the vibration direction of the pump membranes).

The PCB-pump was fabricated with the same technology described in Section 2. The pump chambers were sealed and electrically connected by soldering. The assembly parts are illustrated in Fig. 10. Fig. 11 shows the photographic view of the finished peristaltic pump.

### 3.2. Simulation and characterization

The same simulation tool described in Section 2.3 was also used for modeling the peristaltic pump. We used a simplified model of the pump. The numerical model consists of three pump chambers with three actuating walls. The moving wall condition was used for all three chambers. The peristaltic pump model utilizes the same model for the membrane deflection described in 2.3.

The moving grids are calculated for each pump chamber in every time steps using a user routine written in FORTRAN. Fig. 12 presents the simulation results of the velocity field inside the peristaltic pump. The results show clearly the left-to-right wave motion of the actuators which causes a fluid flow in opposite direction: from right to left.

The same measurement set-up shown in Fig. 6 was used for the characterization of the peristaltic pump. Fig. 13 shows the measured flow rate versus the drive frequency at a constant drive voltage ($V+ = 100$ V, $V- = 0$ V). For frequencies <50 Hz, the flow rate increases proportionally with the frequency. The flow rate reaches its maximum at 50 Hz. The flow rate decreases at higher frequencies because of the large inertia of the fluid in the pump. If the flow rate is controlled by the drive frequency, the operation range should be between 0 and 50 Hz. Smaller pumps with smaller fluid volume will give a wider frequency range.

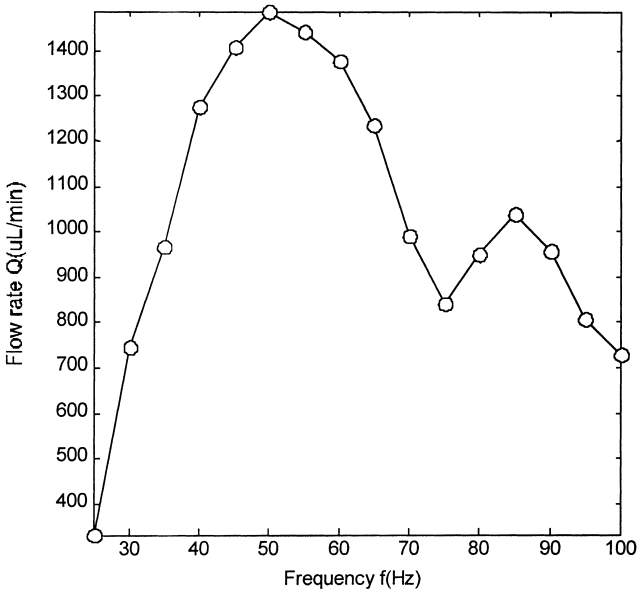


Fig. 13. Flow rate vs. drive frequency (water, $V- = 0$ V, $V+ = 100$ V).

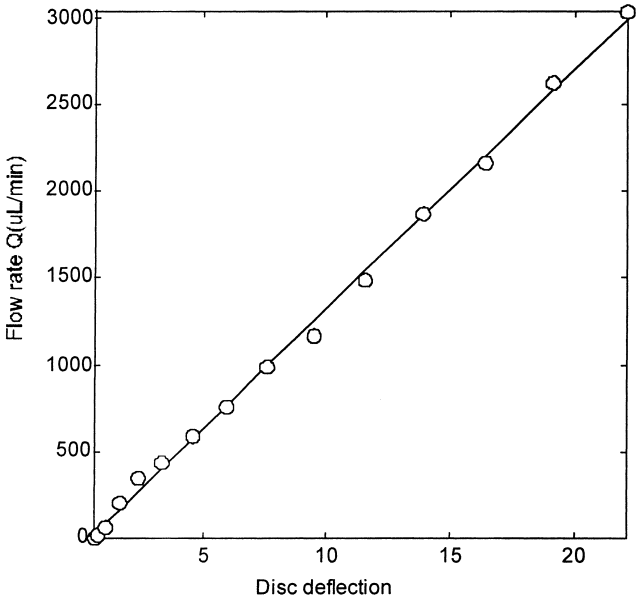


Fig. 14. Flow rate vs. disc deflection (water, $V- = 0$ V, $f = 50$ Hz).

Fig. 14 illustrates the flow rate versus the disc deflection. The circles are measured results. The line is the fitting curve. Comparing the characteristics in Figs. 8 and 14, it is seen that with the same drive voltage, the peristaltic pump delivers higher flow rate. Fig. 15 gives a comparison between the back pressure — flow rate characteristics of the two pumps. At the same drive frequency of 50 Hz and the same drive voltage $V+ = 100$ V, the head loss of the peristaltic pump is 72 cm while the diffuser/nozzle pump can only deliver 38 cm.

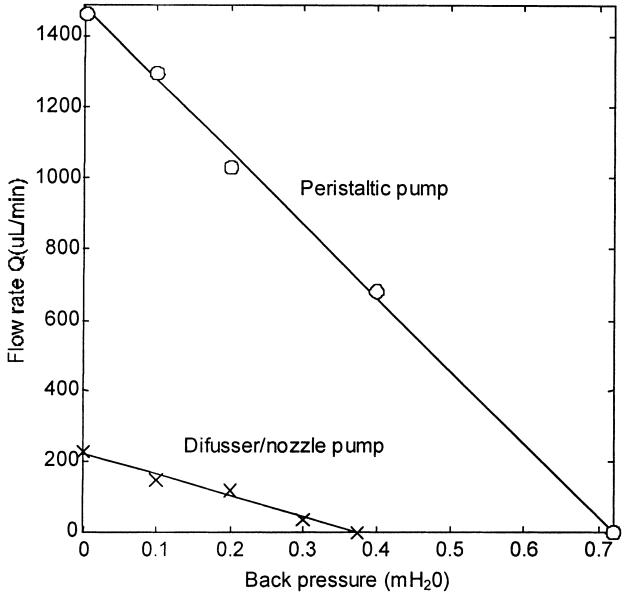


Fig. 15. Back pressure-flow rate characteristics for the two pumps ($V+ = 100$ V, 50 Hz).

## 4. Conclusions

The PCB-based miniature pumps with the piezo discs as the actuators have been developed for a single diffuser/nozzle pump and a peristaltic pump. The results of simulation and characterization have been presented in this paper. It shows that the pumps work well at low frequencies up to 100 Hz for the present design, and they can deliver a maximum flow rate of 3 ml/min.

The results have shown that the use of PCB as substrate material for microfluidic systems is possible and economical. PCB-technology also allows a batch fabrication with lower cost and lower clean room requirements compared to silicon technology. Structure size of around 100 micron is possible with PCB-technology. Therefore, the PCB-technology has a big advantage in system-level integration of microfluidic devices. Interconnecting channels and active fluidic devices as described in this paper can be fabricated easily with a minimal cost. This technique can help to solve the current cost problem caused by expensive packaging of microfluidic devices.

Despite the above-mentioned advantages, PCB-technique is not suitable for complicated devices with small structures which are used to be fabricated with silicon technology. Except the simple examples presented in this paper, element-level integration is hardly to achieve with the traditional PCB-technology.

With some modifications of the current multi-layer PCB-technology, complex and small channel systems can be fabricated by combining the etching technique and the lamination technique. Light-sensitive polymer-based material could extend the machining-ability of PCBs. Further investigation with PCBs based on ceramic substrate and thick film technology promises smaller and more complex sensing and actuating fluidic devices. Traditional techniques like soldering, electroplating, multi-layer lamination and drilling can be used directly for the fabrication of those fluidic devices.

The design methodology for PCB-based systems can be extended to the integration of electronic components and MEMS-components (pressure sensors, mixer, and micro channel, etc.). This new technology promises a low-cost solution for small companies in order to penetrate the promising microfluidics market.

## References

[1] System Planning Corporation, MEMS 1999 — Emerging Applications and Markets, 1999.
[2] MST-News, Microfluidic Systems — New Products, No. 17, October 1996.
[3] S. Shoji, M. Esashi, Microflow devices and systems, J. Micromech. Microeng. 4 (1994) 157–171.
[4] P. Gravesen, J. Branebjerg, O.S. Jensen, Microfluidics — a review, J. Micromech. Microeng. 3 (1993) 168–182.
[5] M. Elwenspoek, T.S. Lammerink, R. Miyake, J.H.J. Fluitman, Towards integrated microliquid handling system, J. Micromech. Microeng. 4 (1994) 227–245.
[6] D.A. Patterson, J.L. Hennessy, Cost and Trends in Cost, in: Computer Architecture — A Quantitative Approach, Morgan Kaufmann, San Francisco, 1997, Chapter 1.4, pp. 18–28.
[7] T.S.J. Lammerink, V.L. Spiering, M. Elwenspoek, J.H.J. Fluitman, A. van den Berg, Modular concept for fluid handling systems: a demonstrator micro analysis system, in: Proceedings of MEMS'96, San Diego, 1996, pp. 389–394.
[8] T. Merkel, M. Graeber, L. Pagel, A new technology for fluidic microsystems based on PCB technology, Sens. Actuators A 77 (1999) 98–105.
[9] I. Moser, G. Jobst, P. Svasek, E. Svasek, M. Varahram, G. Urban, Rapid liver enzyme assay with miniaturized liquid handling system comprising thin film biosensor, Sens. Actuators B 44 (1-3) (1997) 377–380.
[10] L. Lencioni, M.C. Carrozza, A. Menciassi, D. Accoto, N. Croce, P. Dario, A Micromechatronic System for Oil Supply to Momentum Weels Bearing in Space Satellites, Artificial and Natural Perception, World Scientific, Singapore, 1997, pp. 338–342.
[11] J.G. Smits, Piezoelectric micropump with three valves working peristaltically, Sens. Actuators A 40 (1990) 203–206.
[12] Aders Olsson, Valveless Diffuser Micropumps, Ph.D. Thesis, Royal Institue of Technology, Sweden, 1998.
[13] F.K. Forster, L. Bardell, M.A. Afromowitz, N.R. Sharma, A. Blanchard, Design, fabrication and testing of fixed-valve micropumps, in: Proceedings of ASME Fluids Engineering Division, Vol. 234, 1995, IMECE, pp. 39–44.
[14] N.T. Nguyen, R.M. White, Design and optimization of an ultrasonic flexural plate wave micropump using numerical simulation, Sens. Actuators A 77 (1999) 229–236.
[15] N.T. Nguyen, A.H. Meng, J. Black, R.M. White, Integrated flow sensor for in situ measurement and control of acoustic streaming in flexural plate wave micro pumps, Sens. Actuators A 79 (1999) 115–121.
[16] A.E. Herr, J.I. Molho, T.W. Kenny, J.G. Santiago, M.G. Mungal, M.G. Garguilo, Variation of capillary wall potential in electrokinetic flow, in: Proceedings of Tranducers'99, Sendai, Japan, 1999, pp. 710–713.
[17] N.T. Nguyen, X.Y. Huang, Numerical simulation of pulse-widh-modulated micropumps with difusser/nozzle elements, in: Proceedings of International Conference on Modeling and Simulation of Microsystems, San Diego, 2000, 636–639.

## Biographies

*Nam-Trung Nguyen* was born in Hanoi, Vietnam, in 1970. He received the Dipl_Ing and Dr_Ing Degrees in Electronic Engineering from Chemnitz University of Technology, Germany in 1993 and 1997, respectively. In 1998, he worked as a postdoctoral researcher in the Berkeley Sensor and Actuator Center (EECS, University of California at Berkeley). In June 1999, he joined the School of Mechanical and Production Engineering of the Nanyang Technological University in Singapore.

*Xiaoyang Huang* received his BSc in physics in 1982 from Nanjing University, China, and PhD in acoustics in 1989 from Cambridge University, UK. Currently he is an associate professor at School of Mechanical and Production Engineering, Nanyang Technological University, Singapore. His research interest has been in acoustics, unsteady flow control, heat transfer, and now in micro fluidic systems.